

# Analysis of the Epoxy Polymerization Process with Piperidine as the Initiator

Edward A. Aitken

*The Process Group, 79-965 Tangelo, La Quinta, California 92253*

Received 24 March 2005; accepted 15 September 2005

DOI 10.1002/app.23647

Published online in Wiley InterScience (www.interscience.wiley.com).

**ABSTRACT:** Measurements of the rate of heating from a polymerization reaction of a popular Epoxy compound, EPON 828, with piperidine as the initiator were made until no further heat output was detectable. The results were obtained using a microcalorimeter at a temperature of 27.5°C. Three experiments were run where the amine equivalents relative to the epoxy equivalents were 0.034, 0.100, and 0.170. At these ratios, the amine was insufficient to bond with all the epoxide rings. Each amine bond produces an oxide ion, which in turn reacts with other epoxide rings creating another oxide ion. This propagation reaction continues until all the epoxy groups are opened and bonded. The heat rate from the epoxy reaction started at a value proportional to the amine content but then it accelerated rapidly by over an order of magnitude and then decelerated after about 50% completion. The heat rate profiles were found to fit a combination of three mechanisms operating

during the polymerization. The first stage is generation of an oxide ion by amine reaction and by a hydrogen ion exchange between the unreacted amine and a hydroxyl group present in the EPON 828 molecule. The second stage is the rapid acceleration in heat rate due to a build up of an ether bond from the reaction of the oxide ion with an epoxy group. The peak heating rate occurred when the epoxy rings and ether bonds were equal. The last stage is a classic diffusion process, which is the only mechanism left to allow reaction after the other mechanisms have dissipated. The paper generates rate equations and discusses specific issues arising from the heat rate database. © 2006 Wiley Periodicals, Inc. *J Appl Polym Sci* 100: 5066–5086, 2006

**Key words:** epoxy resins; kinetics (polym); calorimetry; cationic polymerization; diffusion

## INTRODUCTION

The Epoxy polymerization process has become a widely used method for bonding and casting plastic entities since its commercial introduction in 1954. Shortly after this introduction, the author<sup>1</sup> studied the process using a basic starting material classified by its developer, Shell Chemical, as Epon 828. Although many other varieties have been created since, Epon 828 has been the reference substance for the study of the reaction kinetics. The 828 product is formed from a reaction of bisphenol with epichlorohydrin and results in an epoxy compound that contains about two epoxy functional groups per molecule. This reaction can be continued to form larger sized molecules depending on the application. The epoxy polymerization must be initiated by adding organic bases such as amines or anhydrides. The type of base influences the reaction rate and other properties as well. For instance, in the case of Epon 828, a primary amine causes a faster rate of polymerization than does a

secondary amine and a much faster rate than that caused by a tertiary amine. Most of the applications use difunctional amine compounds to promote crosslinking. The polymerization reaction is exothermic and may require heating to reach completion in a desired time interval.

Since 1954, the epoxy polymers have become a household word. Studies on the polymerization mechanism are extensive and are summarized in a number of monographs.<sup>2,3,4</sup>

Review of the literature indicates that the reaction kinetics generally follows bimolecular or termolecular rate laws wherein the epoxy group is opened by reaction with the amine. If a hydroxyl group is present it may also provide enhancement of the reaction. Much of the kinetic studies have been done where the reacting functional groups (amine and epoxy) are near the stoichiometric ratio. The implication is that all the opened epoxy groups at completion are attached to amine to provide crosslinking. Yet if the amine initiator is well below the stoichiometric value, the polymerization will continue because of a propagation reaction between the opened epoxy group and other unopened groups forming ether-like bonds.

The analytical tools used for measuring the opening of the epoxy group are extensive. These techniques

Correspondence to: E. A. Aitken (aitkeneaea@aol.com).

include spectrophotometry, differential scanning calorimetry, and electrical conductivity. Calorimetry<sup>5</sup> was used extensively prior to the 1950s to study polymerization rates. Polymerization is usually exothermic and the heat output is a measure of the extent of reaction. For the thesis study a twin type microcalorimeter was used to measure the rate of reaction. It was sensitive to 0.1  $\mu\text{W}$  of power and required only two drops of material. In contrast to other calorimeters which used larger quantities, the microcalorimeter could follow the polymerization to completion as no stirring was required to maintain a uniform temperature. The rate of heat evolution was measured over time instead of the integral heat, providing a more powerful dataset for analysis of the reaction kinetics. The thesis contains all the background experimental information including the design and performance of a twin type calorimeter used to study the reaction rate.

The reaction rates were measured using Epon 828 with piperidine, a monofunctional secondary amine, as the initiator. By using this secondary amine the reaction rates were slow enough that the material could be mixed and incorporated in the calorimeter brought to thermal equilibrium before significant reaction had occurred. The reaction was followed through to its completion for three different amine concentrations. The experiments were performed at 27.5°C in a precisely controlled temperature bath over periods up to 800 h. Within an hour the heat evolution rate could be detected precisely. The reaction had an initial rate that was proportional to the amount of amine added. After a few hours the rate accelerated to a maximum and then diminished to nearly zero heating before the experiment was terminated. The changes in the reaction rate did not follow any of the bimolecular or termolecular rate laws that have subsequently become a popular means of explaining the epoxy polymerization process.

The purpose of this paper is to reexamine the experimental data, expand the mechanistic analysis and propose mechanisms and models that more precisely describe what is happening through all stages of polymerization. With the computerized tools of data processing, not available when the thesis was published, much more can be done. No new experimental data have been generated by the author.

## EXPERIMENTAL

The data showing the heat rate at a time after startup are listed in Table I. Figures 1–3 show graphically the heat rate versus time. Table II shows additional observations computed from the experimental data. Experiment 034 indicates that the ratio of equivalents of the amine group in piperidine is 0.034 that of the equivalents of epoxy in

the mixture. For the other experiments, the ratios were 0.100 and 0.170. Inspection of the figures shows that the overall experimental heating period is shorter with an increase in the amine concentration and that the initial rate of heating increased with amine concentration.

Table III lists the heat rate relative to the maximum value and the calculated integral heat generated at each data point as the fraction of the total. The integral heat was obtained by taking the average of two adjacent heat rates and multiplying the average by the time interval. This incremental heat output was summed cumulatively as the reaction progressed to completion. The cumulative values were then divided by the total heat emitted in the entire experimental period to give a fraction of the heat evolved up to that time. The relative rate was determined by expressing all the heat rates as a fraction of the maximum heat rate observed in the experiment. Figure 4 shows the relative rate versus fraction of heat evolved. Inspection of these figures shows that the 100 and 170 curves are superimposed with no deviation except at the very beginning and very end of the experiment. They both reach a maximum rate at about 53% completion of the total heat evolved. Experiment 034 shows a marked deviation from the others by reaching the maximum rate at about 44% completion. If one displaces the 034 curve by about 7.5%, as shown in Figure 5, superposition occurs with the other experiments except at the start and end of the experiment. Examination of the details of these general observations is reserved for later discussions.

The total heat evolved per equivalents of epoxy was calculated from the data to be, respectively, 13,525, 12,201, and 12,320 cal/equivalent of epoxy for the 034, 100, and 170 experiments. The number of equivalents of epoxy in the three experiments was  $5.3\text{E}-4$ ,  $5.3\text{E}-4$ , and  $4.8\text{E}-4$  respectively. Again the total heat evolved is significantly different in the 034 experiment relative to the other experiments.

## OVERALL REACTION BEHAVIOR

Inspection of the figures shows that the initial heat rate increases with amine concentration. From this start, the reaction rate accelerates to almost 30% completion before starting to decelerate. After passing the maximum rate the rate drops with a convex curvature showing a tail at the very end. In the original thesis the reaction rate was analyzed in terms of second order and third order mechanisms applied to an initiating reaction and a propagating reaction. Neither mechanism matched the experimental curve even when differences in the heat of reaction of the initiating and

**TABLE I**  
**Heat Generation Rates at Various Times of Polymerization**

Experiment 034		Experiment 100		Experiment 170	
$dH/dt$ (cal/h)	Time, $t$ (h)	$dH/dt$ (cal/h)	Time, $t$ (h)	$dH/dt$ (cal/h)	Time, $t$ (h)
0.0029	0.1	0.0114	0.1	0.0181	0.1
0.0029	7.7	0.0114	3	0.0181	5.2
0.0028	9	0.0123	4.5	0.0185	5.7
0.0029	9.7	0.0126	5	0.0183	6.7
0.0029	10.7	0.0124	5.5	0.0187	7.5
0.0029	11.3	0.0121	6.5	0.0201	10.7
0.0029	14.5	0.013	9.5	0.0215	12.7
0.0032	21	0.0134	10.2	0.0219	14.7
0.0038	26	0.0136	12.2	0.0251	18.7
0.0041	31.9	0.0147	13.5	0.0287	22
0.0059	36.9	0.0151	17.5	0.0325	24.7
0.0052	42.2	0.0174	24	0.0356	26.2
0.0053	47	0.0191	27	0.0398	28.7
0.0061	48.3	0.0195	27.7	0.0455	31.5
0.0062	50.1	0.0205	29	0.0563	35
0.0062	51.3	0.0218	30.5	0.0647	37.6
0.0061	55.7	0.0236	33	0.07	38.7
0.0061	62.2	0.0274	36.7	0.074	39.7
0.0063	70.3	0.0332	41.2	0.0894	42.7
0.0069	76.5	0.0373	44.2	0.1142	46.5
0.0073	85.2	0.0445	48	0.1257	48.5
0.0078	96.2	0.0522	51	0.1324	49.5
0.009	104.1	0.0622	54.2	0.1379	50.5
0.0094	110	0.0744	58.1	0.1426	51.2
0.0102	120	0.0888	61.5	0.1459	51.7
0.0119	128.2	0.1068	65.2	0.1495	52.7
0.0123	131.6	0.1205	68.5	0.1529	54
0.0149	142.3	0.133	73	0.1534	54.2
0.0164	147.8	0.1349	74.8	0.1545	55
0.0177	152.2	0.1315	77.5	0.1545	55.5
0.0178	153.1	0.1294	78.5	0.1538	56
0.0189	157	0.1218	80.7	0.1524	56.5
0.0236	167.7	0.1161	81.7	0.1462	58.2
0.0261	171.8	0.0991	84.7	0.1453	58.5
0.0298	179.3	0.0939	85.7	0.1408	59.5
0.0358	191.8	0.0856	87	0.1338	60.2
0.0391	199.2	0.0646	90.9	0.1323	60.5
0.041	204.2	0.05	94.5	0.1203	62
0.0431	214.7	0.0407	97.5	0.1122	63
0.0429	223	0.0348	99.7	0.0818	66.5
0.0425	229.2	0.0291	102.7	0.0589	69.7
0.0399	238.3	0.0186	109.7	0.0451	73
0.0369	244.7	0.0114	121	0.0386	74.7
0.0333	252	0.0078	131.7	0.0345	76
0.0282	262.3	0.0053	143.7	0.0259	79.5
0.025	268.7	0.0041	155.5	0.0214	82.7
0.0216	276.9	0.003	167.7	0.0161	87
0.0176	287.2	0.0024	195	0.0104	96.3
0.0159	293.2	0.0023	195.2	0.0086	101.7
0.0141	300.2	0.0015	216	0.0066	109
0.0116	312.2	0.0011	244	0.0047	123
0.0101	320.7	0.0007	267	0.0034	135
0.0083	334.8	0.0003	297	0.0029	151.2
0.0074	343.3			0.0019	173.7
0.0057	364.5			0.0013	216.7
0.0047	387			0.0013	217.7
0.004	410.5			0.001	243.7
0.003	440			0.0006	270
0.0021	490				
0.0015	561				
0.0017	575.5				
0.0015	632				
0.0011	673				
0.0007	823				

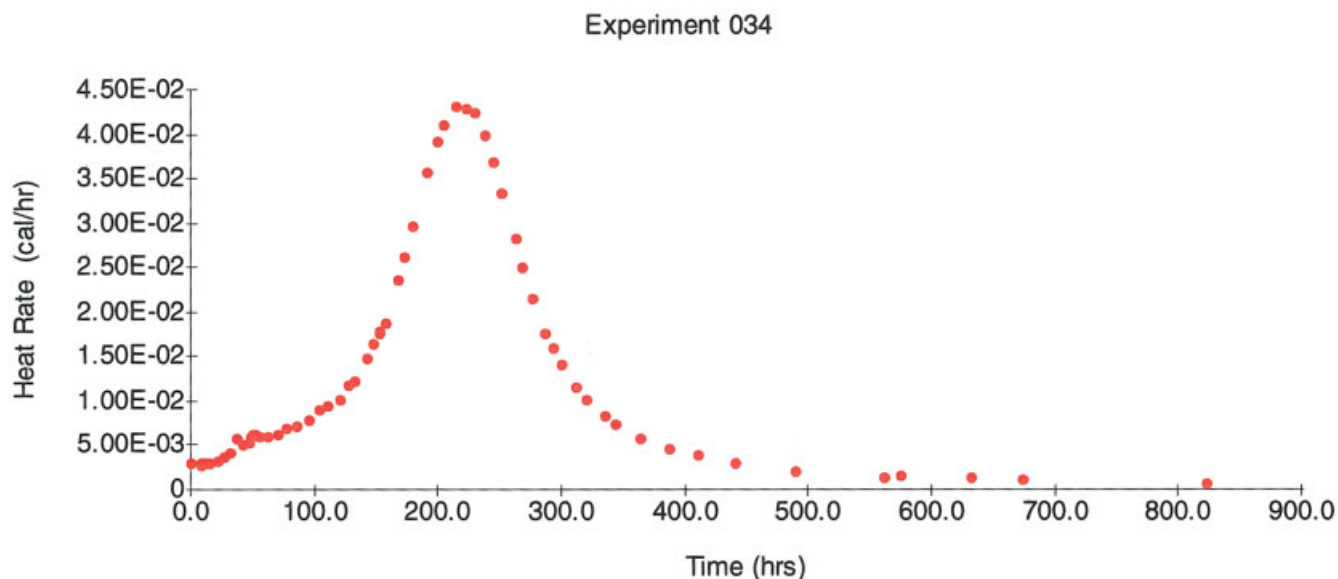


**Figure 1** Heat rate versus time Experiment 034. [Color figure can be viewed in the online version, which is available at [www.interscience.wiley.com](http://www.interscience.wiley.com).]

propagating steps were taken into account. These mechanisms could not produce an *accelerating* rate that was evident in the experiments.

The thesis revealed two compelling empirical observations about the reaction rates. One observation was that during the initial stages up to about 30% completion, the reciprocal of the heat rate was proportional to

the time with a slope that was about the same for all three amine concentrations. The second observation was that after about 70% completion the heat rate in all three experiments diminished proportional to the 1.5 power of the time. Neither of these findings could be explained from purely concentration terms of the reactive species. This paper examines these observa-

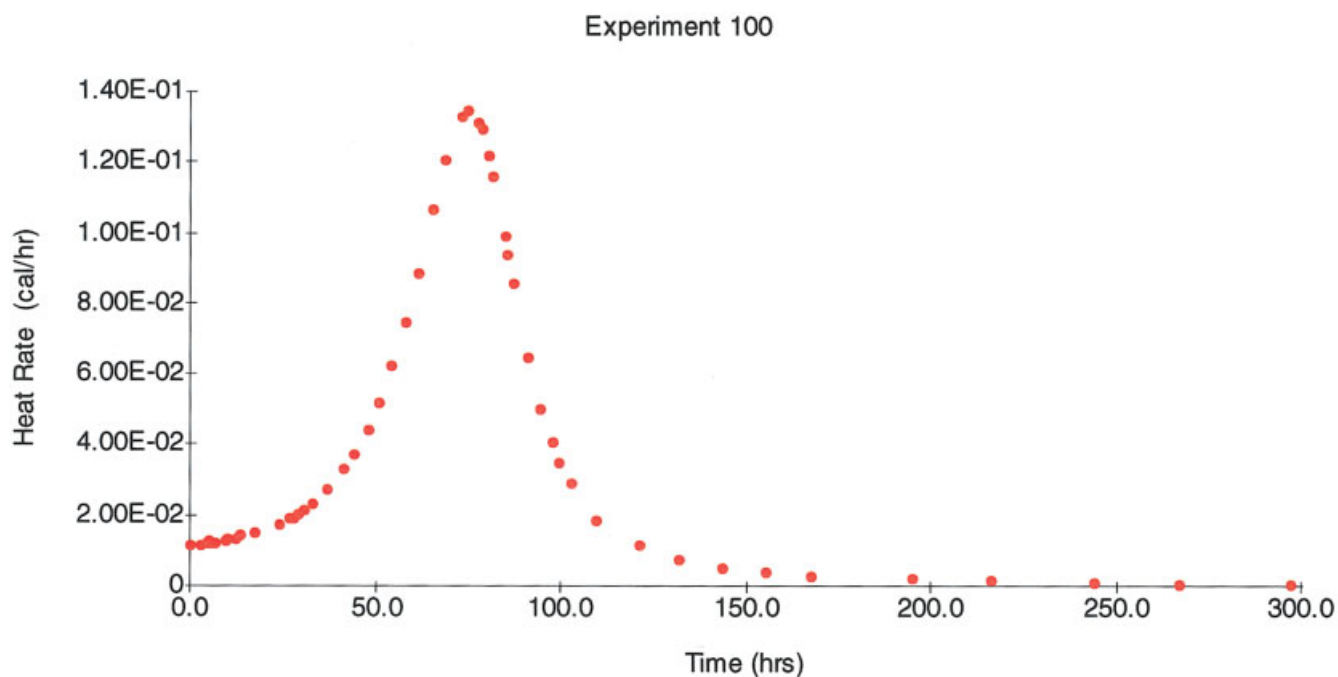


**Figure 2** Heat rate versus time Experiment 100. [Color figure can be viewed in the online version, which is available at [www.interscience.wiley.com](http://www.interscience.wiley.com).]

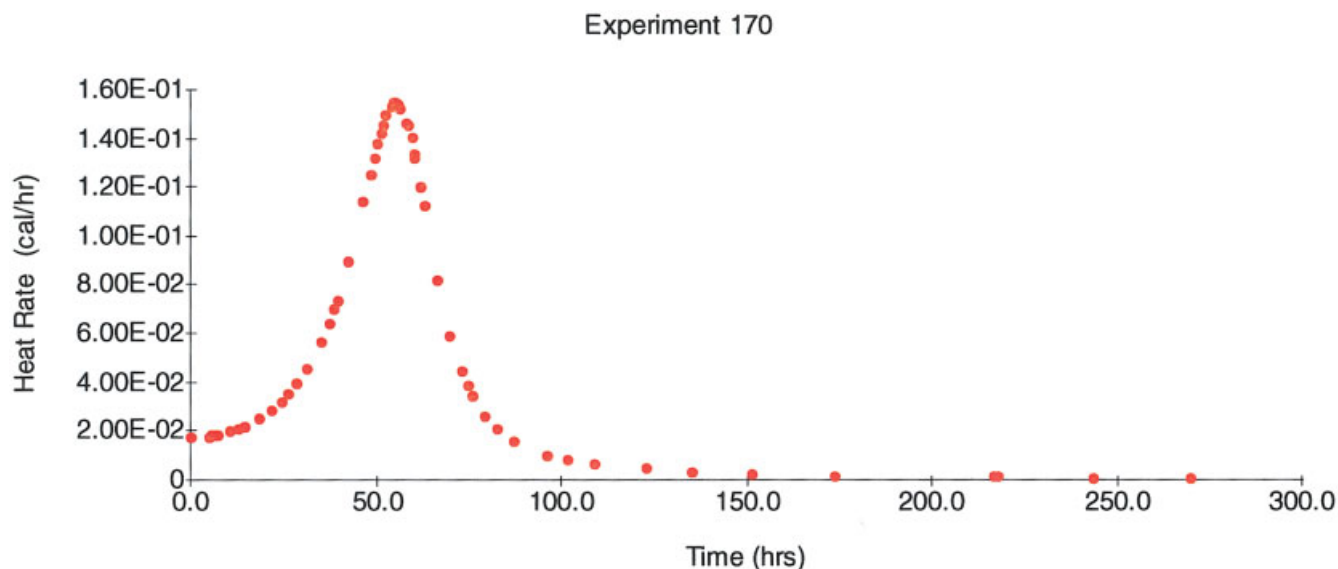


**Figure 3** Heat rate versus time Experiment 170. [Color figure can be viewed in the online version, which is available at [www.interscience.wiley.com](http://www.interscience.wiley.com).]

tions in detail and proposes a reaction rate consistent with the empirical findings.

The premise for this new analysis is based on the following reactions. The initiating step requires opening an epoxide ring and creating an oxide ion: (1) by bonding the amine to a carbon atom of the epoxy group or (2) by acid–base equilibration by exchange of a hydrogen ion between a hydroxyl group in the epoxy molecule and the amine converting it to an aminium ion. The opening of the epoxide ring reaction with the amine is expected to be exothermic but possibly different than the opening by an oxide ion during the propagating stage. The heat evolved from the acid–base equilibration, option (2) is instantaneous and not exothermic. The propagating step is the reaction of the oxide ion with another epoxy group to form an ether-like bond and a new oxide ion. This reaction continues until all epoxy groups are opened and bonded.

The polymerization is carried out in an environment of oxide ions, which is apparent from an increase in the electrical conductivity during the propagating stage.

The analysis to follow will be divided into two phases: the initial or accelerating period up to the maximum and the decelerating phase beyond the maximum. The transition from the accelerating phase to the decelerating phase will be discussed last. There obviously is more than one mechanism operating and knowing what triggers the transition will be an important outcome of this analysis.

#### DISCUSSION AND ANALYSIS OF THE ACCELERATING PHASE

The initial heat rate, as expected, is proportional to the amine concentration. However a detailed examination

**TABLE II**  
Key Observations From the Polymerization Study

Observation	Experiment		
	034	100	170
Equiv. epoxy at $T(0)$	5.3E–4	5.3E–4	4.8E–4
Equiv. amine at $T(0)$	1.8E–5	5.3E–5	8E–5
Equiv. hydroxyl at $T(0)$	5.3E–5	5.3E–5	4.8E–5
Total heat generated (cal)	7.27	6.47	5.91
Heat/equiv. epoxy (cal)	13500	12200	12300
Time (h) at max heat rate	215	74.8	55.2
Max. heat rate (cal/h)	43.1E–3	134.9E–3	154.5E–3
Fraction heat at max heat rate	0.44	0.53	0.53
Initial heat rate	2.9E–3	11.4E–3	18.1E–3
Duration of experiment (h)	823	297	270

**TABLE III**  
**Relative Heat Generation Rates versus Fraction of Total Heat Evolved**

Experiment 034		Experiment 100		Experiment 170	
Rate	Heat	Rate	Heat	Rate	Heat
0.067	0.000	0.085	0.000	0.117	0.000
0.067	0.003	0.085	0.005	0.117	0.016
0.065	0.004	0.091	0.008	0.120	0.017
0.067	0.004	0.093	0.009	0.118	0.021
0.067	0.004	0.092	0.010	0.121	0.023
0.067	0.005	0.090	0.012	0.130	0.034
0.067	0.006	0.096	0.018	0.139	0.041
0.074	0.009	0.099	0.019	0.142	0.048
0.088	0.011	0.101	0.023	0.162	0.064
0.095	0.014	0.109	0.026	0.186	0.079
0.137	0.018	0.112	0.035	0.210	0.093
0.121	0.022	0.129	0.052	0.230	0.101
0.123	0.025	0.142	0.060	0.258	0.117
0.142	0.026	0.145	0.062	0.294	0.138
0.144	0.028	0.152	0.066	0.364	0.168
0.144	0.029	0.162	0.071	0.419	0.194
0.142	0.033	0.175	0.080	0.453	0.207
0.142	0.038	0.203	0.095	0.479	0.219
0.146	0.045	0.246	0.116	0.579	0.260
0.160	0.051	0.277	0.132	0.739	0.326
0.169	0.060	0.330	0.156	0.814	0.366
0.181	0.071	0.387	0.178	0.857	0.388
0.209	0.081	0.461	0.207	0.893	0.411
0.218	0.088	0.552	0.248	0.923	0.428
0.237	0.102	0.658	0.291	0.944	0.440
0.276	0.114	0.792	0.347	0.968	0.465
0.285	0.120	0.893	0.405	0.990	0.498
0.346	0.140	0.986	0.493	0.993	0.503
0.381	0.152	1.000	0.530	1.000	0.524
0.411	0.163	0.975	0.586	1.000	0.537
0.413	0.165	0.959	0.606	0.995	0.550
0.439	0.175	0.903	0.649	0.986	0.563
0.548	0.207	0.861	0.667	0.946	0.606
0.606	0.221	0.735	0.717	0.940	0.614
0.691	0.250	0.696	0.732	0.911	0.638
0.831	0.307	0.635	0.750	0.866	0.654
0.907	0.346	0.479	0.795	0.856	0.661
0.951	0.374	0.371	0.827	0.779	0.693
1.000	0.436	0.302	0.848	0.726	0.712
0.995	0.485	0.258	0.861	0.529	0.770
0.986	0.522	0.216	0.876	0.381	0.808
0.926	0.575	0.138	0.902	0.292	0.837
0.856	0.609	0.085	0.928	0.250	0.849
0.773	0.645	0.058	0.944	0.223	0.857
0.654	0.689	0.039	0.956	0.168	0.875
0.580	0.713	0.030	0.965	0.139	0.888
0.501	0.739	0.022	0.971	0.104	0.901
0.408	0.767	0.018	0.983	0.067	0.922
0.369	0.781	0.017	0.983	0.056	0.931
0.327	0.796	0.011	0.989	0.043	0.940
0.269	0.818	0.008	0.994	0.030	0.954
0.234	0.831	0.005	0.998	0.022	0.962
0.193	0.849	0.002	1.000	0.019	0.970
0.172	0.858			0.012	0.980
0.132	0.877			0.008	0.991
0.109	0.894			0.008	0.991
0.093	0.908			0.006	0.996
0.070	0.922			0.004	1.000
0.049	0.940				
0.035	0.958				
0.039	0.961				
0.035	0.974				
0.026	0.981				
0.016	1.000				



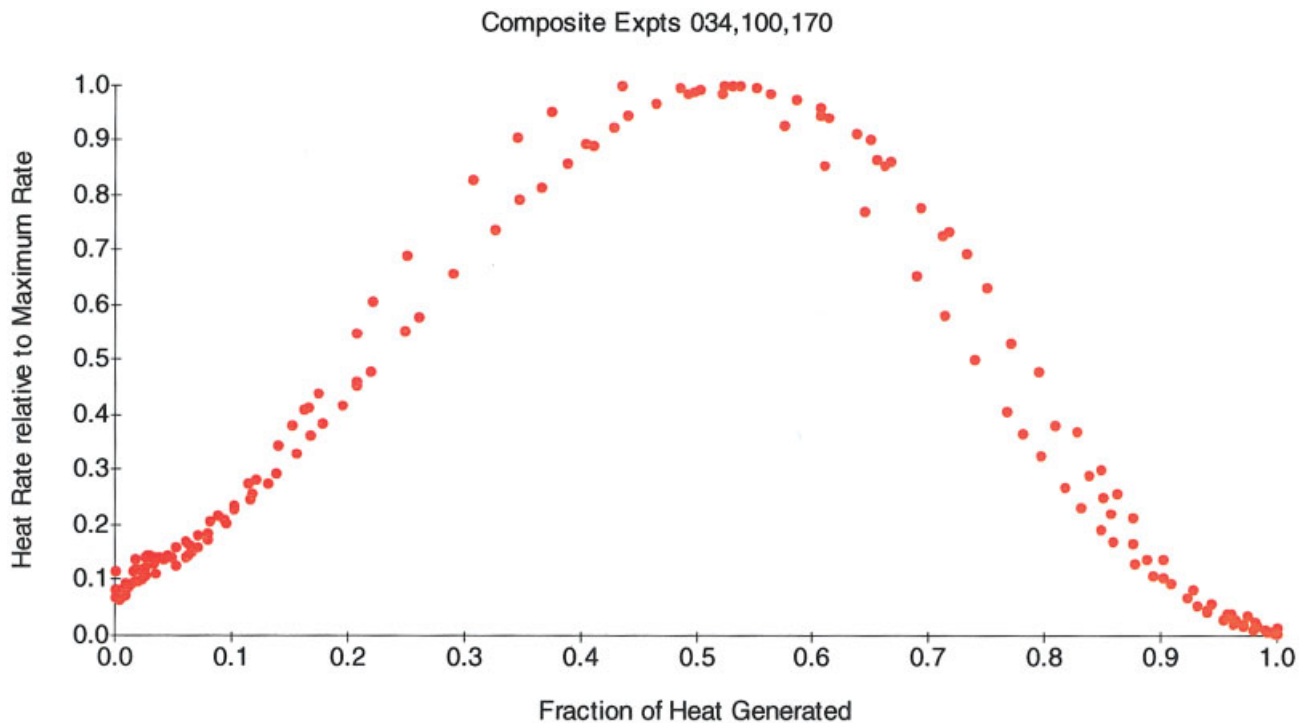


**Figure 4** Heat rates versus heat generated. Composite expts 034, 100, 170. [Color figure can be viewed in the online version, which is available at [www.interscience.wiley.com](http://www.interscience.wiley.com).]

of the data points in the early stages reveal a more intricate set of findings. First, the data points up to 30% of completion are plotted in the form of reciprocal of the heat rate versus time. There is a strong linear dependence except at the very start of the experiment and holds up to  $\sim 30\%$  where an inevitable deviation

from linearity would be expected. To give a precise curve fit to this linearity, the initial and last data points that showed deviation were rejected until the lowest standard error was obtained in a regression analysis. This exercise produced the curves shown in Figures 6–8 for the three amine concentrations.

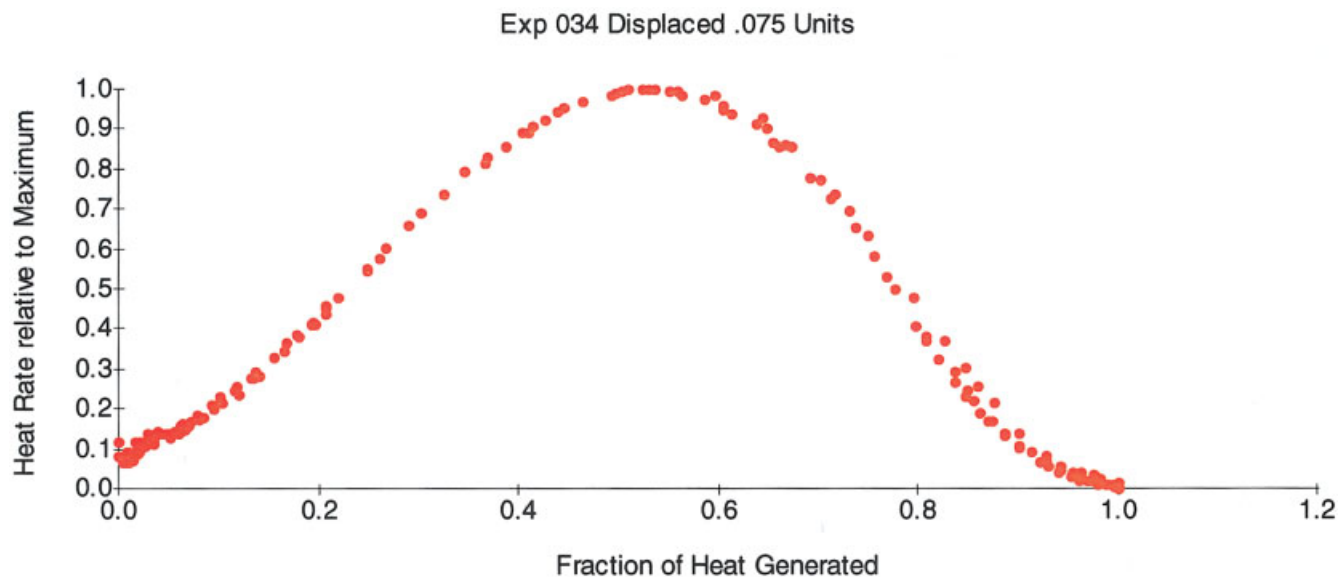


**Figure 5** Heat rates versus heat generated Experiment 034 displaced 0.075 units. [Color figure can be viewed in the online version, which is available at [www.interscience.wiley.com](http://www.interscience.wiley.com).]

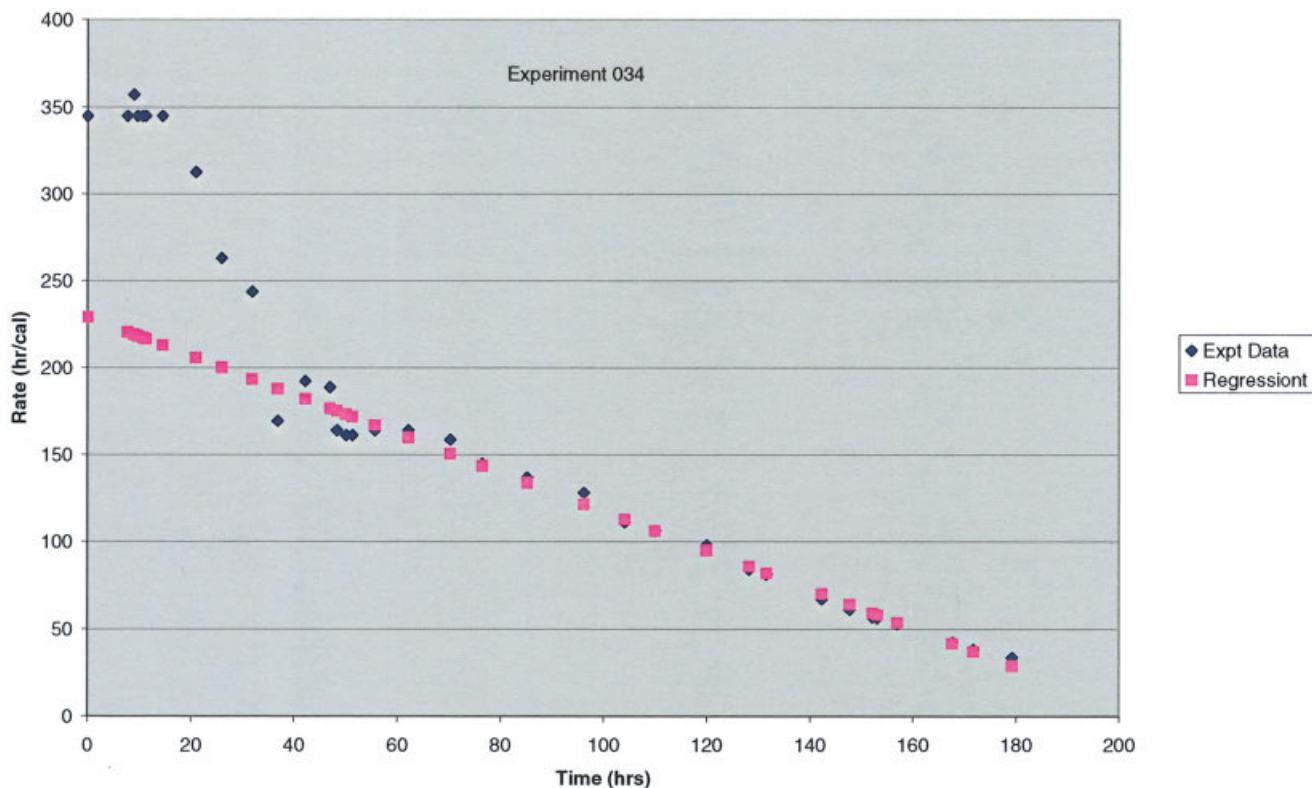


**Figure 6** Reciprocal rate versus time. [Color figure can be viewed in the online version, which is available at [www.interscience.wiley.com](http://www.interscience.wiley.com).]

For the 034 Experiment (see Fig. 6), there was a relatively long period ( $\sim 40$  h) where the heat rate was significantly below the value indicated by extrapolation of the linear regression to zero time. The regression yielded the following equation:

$$[dH/dt]^{-1} = -1.12t + 229.3$$

The intercept is 229.3 h/cal but the original reciprocal heat rate was about 348. In the period up to 40 h, the reciprocal heat rate declined rapidly to the linear regression curve and followed it thereafter up to about 180 h. This situation indicates a possible change in the mechanism during the accelerating phase.

For the 100 Experiment (see Fig. 7), there was only a slight difference in the initial reciprocal heat rate ( $\sim 88$ ) and the intercept derived from a regression analysis of subsequent data points out to 55 h. The linear regression yielded the following equation:

$$[dH/dt]^{-1} = -1.39t + 89.2$$

The intercept, 89.2, is only slightly larger than the observed initial value of 88. The observed value was

constant for about 5 h before the data started to follow the linear regression curve.

For the 170 Experiment (see Fig. 8), the initial reciprocal heat rate was less than the intercept of the least square fit of the subsequent data points out to 2 h. The regression analysis in this case yielded the following equation:

$$[dH/dt]^{-1} = -1.26t + 62.5$$

This exercise indicates there is a relationship between the amine concentration and the differences between observed initial heat rates and the extrapolated heat rates from the regression analyses of the accelerating phase of the reaction. The coefficients of the time dependence appear to be reasonably constant and independent of the amine concentration however. From this data set, two separate correlations can be derived, both proportional to the amine concentration. At  $t = 0$ , the heat rate is merely the reciprocal of the intercept in the three linear curves derived above. If these values are plotted against the initial amine concentration,  $A_0/M_0$ , there is a good linear fit as shown in Figure 9. A regression analysis of the three amine contents shows only small deviations from the calculated value. The regression treatment of the three data points was calculated to be:



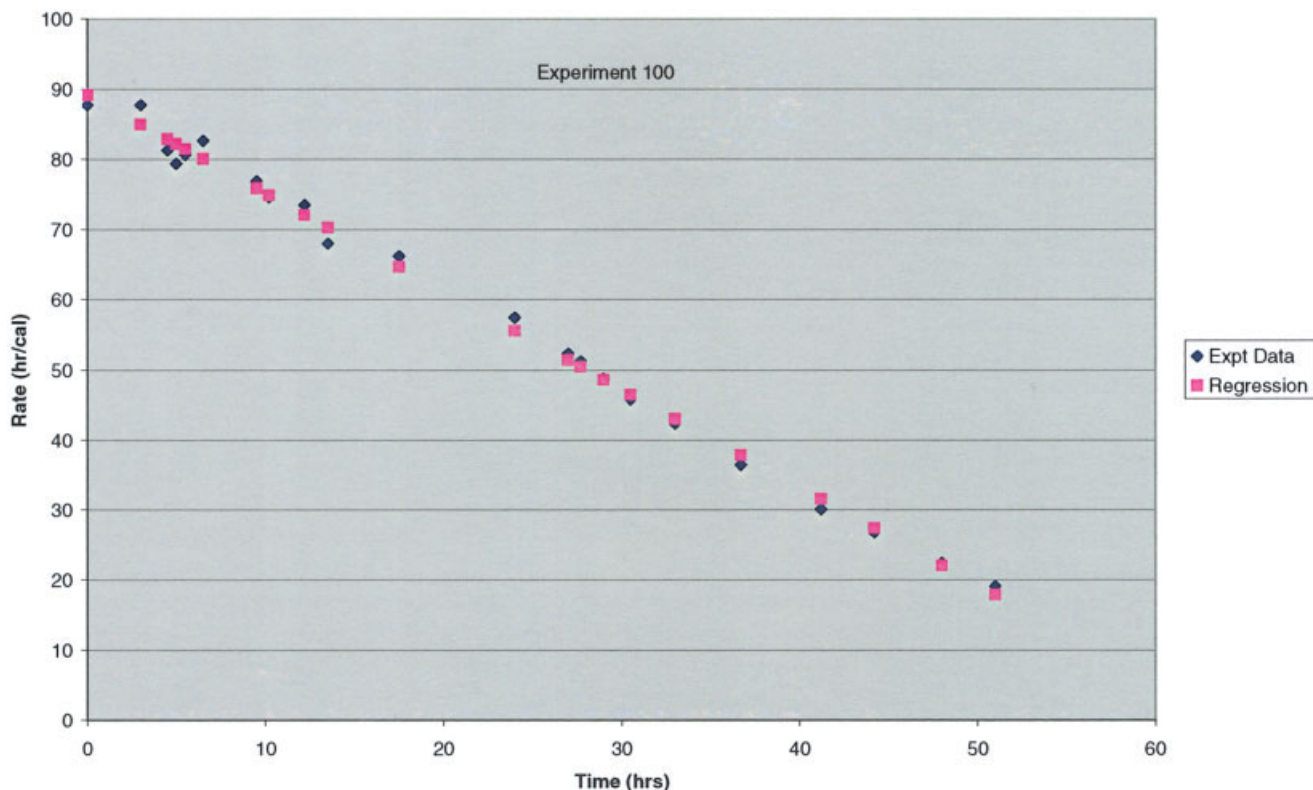


**Figure 7** Reciprocal rate versus time. [Color figure can be viewed in the online version, which is available at [www.interscience.wiley.com](http://www.interscience.wiley.com).]

$[dH/dt \text{ at } t = 0 \text{ by extrapolation}]$

$$= 0.0854A_0/M_0 + 0.00187$$

where  $A_0$  and  $M_0$  are the equivalents of amine and epoxy at  $t = 0$ .

Since the measured initial heat rates differed from these back extrapolated rates, it would appear that another mechanism is operating in certain situations. To determine this correlation, the difference in the initial measured heat rate and the extrapolated heat rate calculated above is plotted against the amine concentration and shown in Figure 10. Again a good linear fit is obtained and the regression analysis produced the following relation:

$$[dH/dt \text{ at } t = 0 \text{ by measurement}] - [dH/dt \text{ at } t = 0 \text{ by extrapolation}] = 0.0268A_0/M_0 - 0.00241$$

By combining these two equations, the result for the initial measured heat rate is:

$$[dH/dt \text{ at } t = 0 \text{ by measurement}] = 0.1122A_0/M_0 - 0.00054 \quad (1)$$

The last term in this equation is very small and may be the residual in the error of the measurements.

The analysis reveals two heat producing mechanisms. If  $A_0/M_0 < 0.100$ , the initial heat rate results from a reaction of amine and the epoxy group. If  $A_0/M_0 > 0.100$ , the initial heat rate is dominated by the reaction mechanism operating during the accelerating phase. When the amine concentration exceeds a certain threshold then the accelerating mechanism takes off at  $t = 0$  and the initial condition for its dominance is created instantaneously. On the other hand, below this threshold, it cannot operate until a sufficient amount of reaction of amine with epoxy groups has occurred. This direct reaction results in the formation of an oxide ion. It would appear that a sufficient concentration of oxide ions must be present before the accelerating mechanism can take off. There is a time period before this condition can be achieved. Inspection of the 034 Experiment shows that almost 40 h is required before the accelerating mechanism becomes dominant. For 100 Experiment, the time period was the order of a few hours at most.

The accelerating mechanism is influenced by the amine concentration only in establishing the initial threshold condition. The intercept of the linear fit was

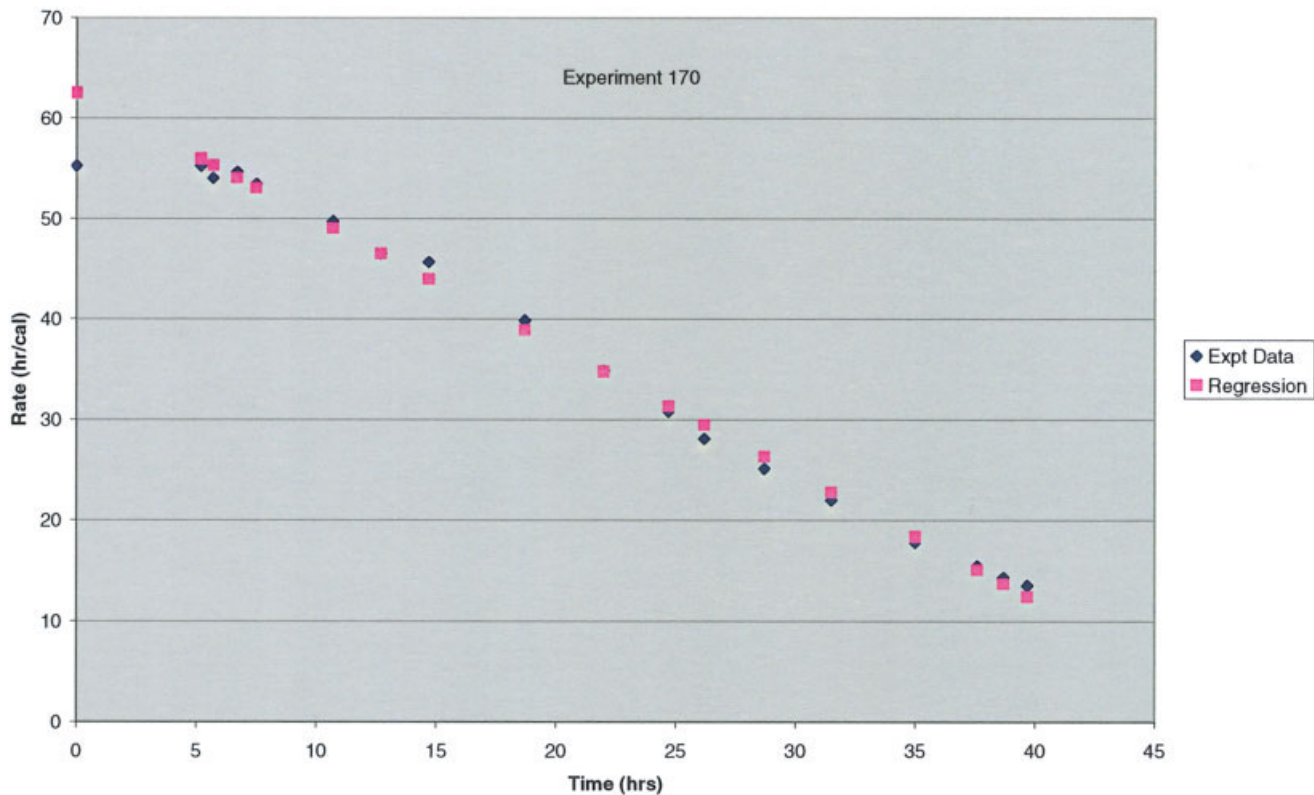


Figure 8 Reciprocal rate versus time. [Color figure can be viewed in the online version, which is available at [www.interscience.wiley.com](http://www.interscience.wiley.com).]

proportional to the amine concentration thereafter the time dependent portion (slope) of the change of the heat rate was independent of the amine concentration. This indicates that the amine acts instantaneously. A

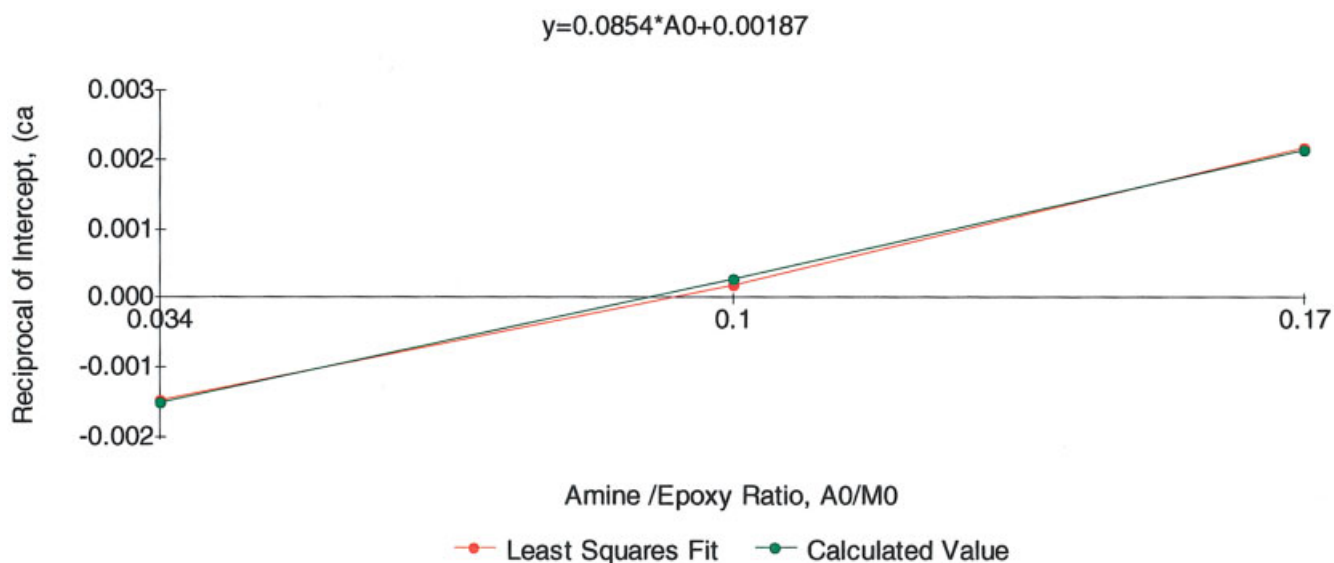
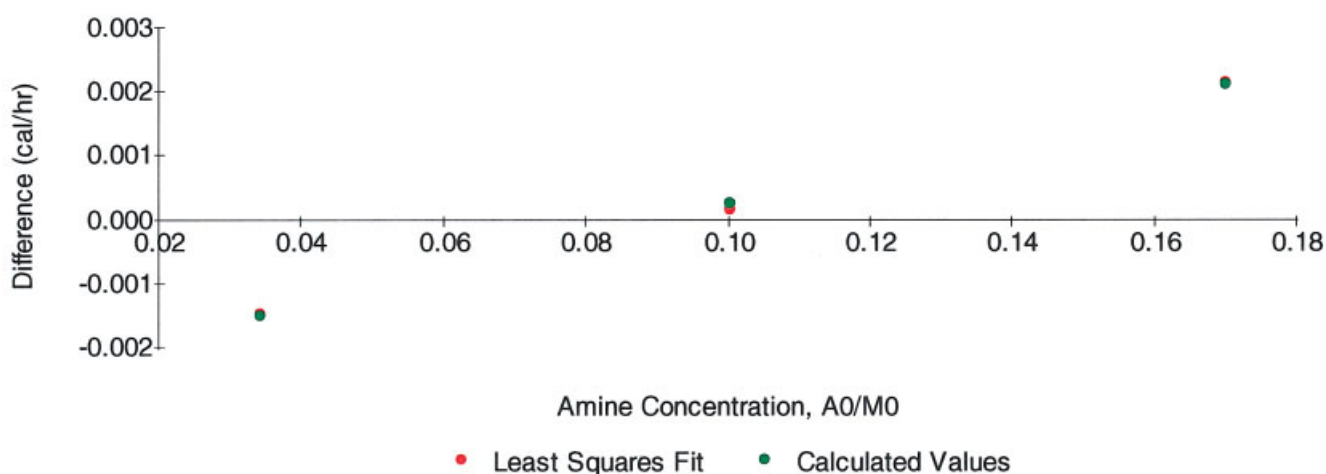


Figure 9 Intercept versus amine content. [Color figure can be viewed in the online version, which is available at [www.interscience.wiley.com](http://www.interscience.wiley.com).]

**Fig 4.5 Deviations @ T=0 vs A0/M0**

$$y=0.0268 \cdot A_0 - 0.00241$$



**Figure 10** Deviations at  $T = 0$  versus  $A_0/M_0$ . [Color figure can be viewed in the online version, which is available at [www.interscience.wiley.com](http://www.interscience.wiley.com).]

reasonable explanation would be that oxide ions are created by acid–base exchange of the amine with the hydroxyl groups in the epoxide molecule. The mass action law would support the observation that the amount of oxide ions from this exchange would be proportional to the amine concentration as shown in the analysis.

The mass action law would be instantaneous, evolve little or no heat and its influence would be governed by an equilibrium constant,  $K$ . The reaction of an amine with the epoxy group would be a slower process, evolve some heat and its influence would be governed by a rate constant,  $k$ , for a bimolecular reaction. The amine reaction could continue simultaneously with the accelerating mechanism and would dissipate as the availability of unreacted (or unexchanged) amine or unreacted epoxy groups is diminished. With this premise several implications can be derived from the data.

#### Derivation of the equilibrium constant, $K$

The equivalents of oxide ion can be calculated from the starting amounts of reactants in the acid–base exchange reaction:



The reaction products: aminium and oxide ion contents are equal. In Table IV the oxide ion content is shown for three amine concentrations based on an equilibrium constant of 0.0215. This value is dependent on the hydroxyl content which is assumed to be

0.1 of the epoxy content. The selection of this value for  $K$  will be evident later. From application of the mass action formula, the oxide ion content increases with amine content but is only 10–20% of the initial amine content.  $K$  and the hydroxyl content are complementary so that if one is changed the other must change in the opposite direction.

#### Derivation of the rate constant, $k$

The equivalents of oxide ion produced by a bimolecular reaction between the amine and the epoxy group can be calculated from a rate constant and the initial heat rate at  $t = 0$  determined by the regression analysis. In Table V the calculated rate constant is reasonably consistent from the three amine experiments

The initial heat rate is calculated from eq. (1) for each amine concentration. The heat rate is divided by the heat of reaction per equivalent of amine, assumed to be 14,000 cal and the result is  $k$ , in units of equiva-

**TABLE IV**  
Determination of Oxide Ion and Equilibrium Constant From Data at  $T = 0$

	Experiment No.		
	034	100	170
Equiv. epoxy	5.3E–4	5.3E–4	4.8E–4
Equiv. amine	1.80E–5	5.3E–5	8.2E–5
Equiv. hydroxyl	5.3E–5	5.3E–5	4.8E–5
Equiv. oxide ion	3.86E–6	6.77E–6	7.96E–6
$K$	0.0215	0.0215	0.0215

TABLE V  
Determination of Oxide Ion and Rate Constant of  
Amine-Epoxy From Regression Data at  $t = 0$

	Experiment No.		
	034	100	170
Eq. (1) slope	0.112	0.112	0.112
Eq. (1) intercept	-0.00054	-0.00054	-0.00054
$dH/dT$ at $t = 0$ (cal/h)	0.00327	0.0107	0.0185
Heat of Rx (cal/equiv)	14000	14000	14000
K	0.0165	0.0165	0.0180
Rx time, $t_a$ , prior to acceleration (h)	30	5	2
Equiv. oxide ion at $t_a$	7.04E-6	4.20E-6	2.88E-6

lents per hour. Since the epoxy content is much larger than the amine, it is constant when applied over short time periods after initiation. The oxide ion is produced by reaction of the amine and accumulates over the period before the acceleration mechanism starts. The accumulation follows a semibimolecular term,  $A_0/M_0(1 - \exp(-kt_a))$ . The last row in Table V shows that the calculated oxide ion content decreases with increasing amine content. This trend is opposite to the oxide content produced by the acid-base exchange shown in Table IV. The values for  $k$  and heat of reaction are complementary also.

#### Determination of the oxide ion content at onset of acceleration

The total oxide ion content in the polymer is the sum of the contents listed in Tables IV and V. Table VI shows the total oxide content at the onset of the accelerated mechanism,  $t_a$ . Remarkably, the values are essentially the same at all amine concentrations. This supports the premise that the accelerating mechanism cannot occur until the ion concentration reaches a threshold. This threshold is fairly insensitive to the choices of complementary parameters assumed in the calculation. Increasing the heat of reaction from 14,000 to 18,000 and increasing the hydroxyl content from 0.1 to 0.2 of the epoxy con-

tent causes less than a few percent change in the total oxide ion content.

From the density (1 g/cc), and the molecular weight (350) the oxide ion spacing can be estimated in terms of a cubic array. One oxide ion would share the corners of the cube with sides of about 25 Å. One epoxy group would be spaced in a cubic array of about 6.9 Å. If the reaction of amine with epoxy is carried fully to completion, the maximum possible oxide ion content would be equal to the initial amine content and the spacing between nearest neighbor would decrease below 25 Å as shown in the last row of Table VI.

The dominance of the mass action law at high amine concentrations could explain the lower integral heat evolved in Experiments 100 and 170 relative to Experiment 034 as the result of its greater use in nonheat producing reactions.

So far the discussion of the accelerating phase has been limited to the initial conditions for its occurrence. A reasonable explanation is that the oxide ion content in the material must be at a certain level to allow the reaction rate to accelerate. The reaction of oxide ion with epoxy groups regenerates the oxide ion but it cannot explain acceleration by a bimolecular reaction mechanism. Therefore there must be a change in a property of the system. The property proposed is the electrical conductivity that is made possible by the existence of oxide ions. There is a strong chemical potential for reaction between the amine/oxide ion and the epoxy. With this potential and the close proximity of these reactants, the reaction rate can be influenced by the electrical field rather than by diffusion or reaction rate constants particularly in the early stages of the polymerization. This situation is analogous to oxidation of metals when the oxide layer is the order of 100 Å. The field established by the chemical potential is strong enough to pull the oxide ion through the oxide layer at much faster rates than would be expected by diffusion. As the oxide layer grows the field effects diminish and the oxidation rate reverts to a diffusion-controlled mechanism. The premise in the discussion to follow will be that the conductivity is the

TABLE VI  
Determination of Oxide Ion Contents and Mean Spacing Between Nearest Neighbors  
in a Cubic Array

	Experiment No.		
	034	100	170
Total oxide ion at $t_a$	10.90E-6	10.98E-6	10.84E-6
Mean spacing in a cubic array, $A^0$	25.2	25.2	24.5
Mean spacing of the epoxy, $A^0$	6.9	6.9	6.9
Max. possible oxide ion in system	18E-6	53E-6	80E-6
Mean spacing of max. oxide array	21.3	14.9	12.6

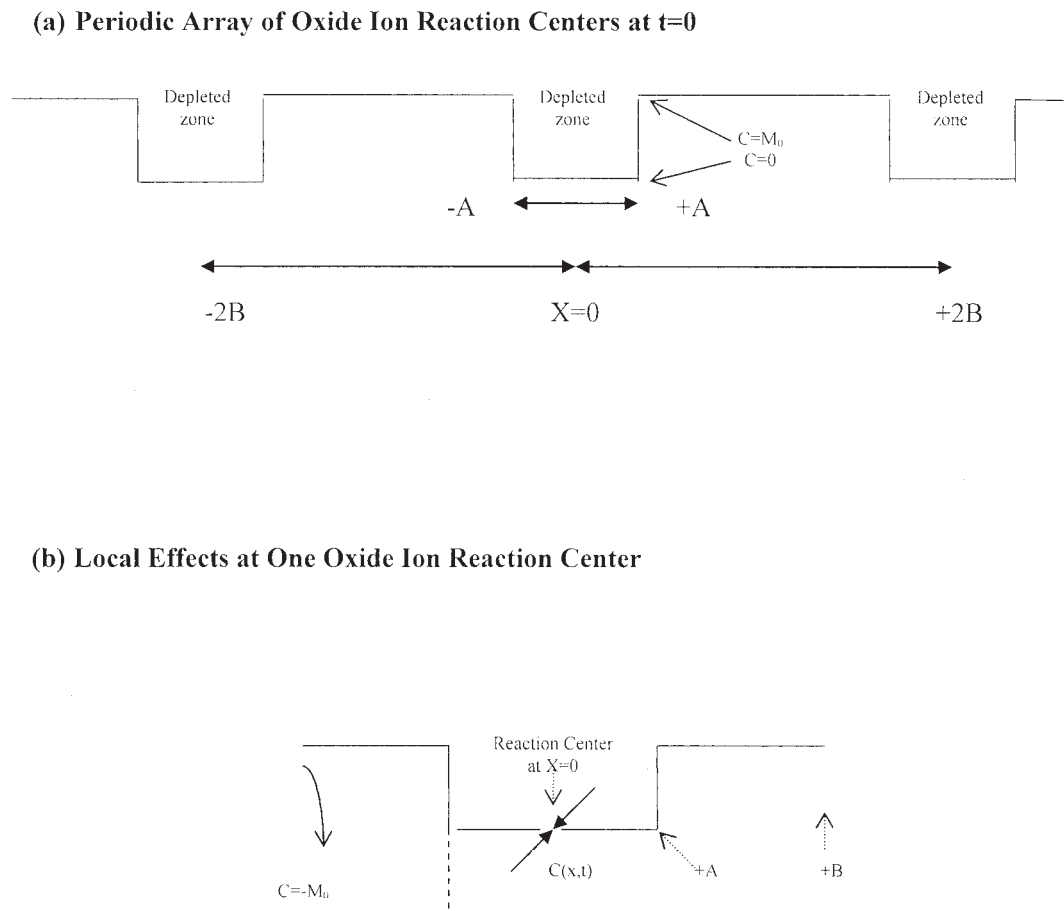


**Figure 11** One dimensional schematic of the diffusion model. (a) Periodic array of oxide ion reaction centers at  $t = 0$ . (b) Local effects at one oxide ion reaction center. Epoxy ring diffuses to oxide ion at  $x = 0$ , reacts with it and vanishes regenerating a new oxide ion. The reaction can be simulated mathematically by transposing one side to  $C = -M_0$ . The diffusion stream from the left is offset by the stream from the right side and  $C = 0$  at  $x = 0$ ,  $t > 0$ .  $C(x,t)$  = Fraction of  $M_0$  at  $x$  and  $t$ : Calculated from 4 error functions( $x, t$ ) with parameters  $A$  and  $B$ .  $dC(0,t)/dt$  = Rate of arrival of epoxy rings at  $x = 0 \approx$  Heat rate from diffusion model.  $dC(0,t)/dt = \{C(\delta x, t_1) - C(\delta x, t_2)\}/(t_1 - t_2)$ .  $\delta x$  is a small incremental distance from  $x = 0$ :  $\delta x \ll B$ .  $t_1, t_2$  are successive time measurements.

property undergoing change. Changes in the oxide ion concentration, increases the conductivity and accelerates the reaction rate. The rate increases monotonically until the system is exhausted with epoxy groups that are sufficiently close to pull in the oxide ion or amine group. Thereafter the reaction rate is controlled by diffusion processes that can operate over longer distances.

#### DISCUSSION AND ANALYSIS OF THE DECELERATING PHASE

The thesis noted that an empirical relationship between the heating rate and the time followed a 3/2 power dependence for all three amine concentrations for values obtained after 70% of the heat was generated. It is well known that diffusion processes exhibit this type of time dependence so that such would not

be unexpected in epoxide polymerization. After gelation and extensive depletion of the epoxide groups, the oxide ion may be far removed from unopened epoxide and diffusion kinetics would be appropriate. In fact diffusion should be operating from the beginning and should be a competing mechanism during the entire propagation stage of the polymerization. To establish the heat rate from a pure diffusion standpoint, a diffusion model was constructed to compare with the experimental results.

#### Proposed diffusion model

During propagation the oxide ion is regenerated with an opening of the epoxide ring. The ion can be viewed as permanently located along a one dimensional line spaced periodically at a distance of  $2B$  units where  $B$  is



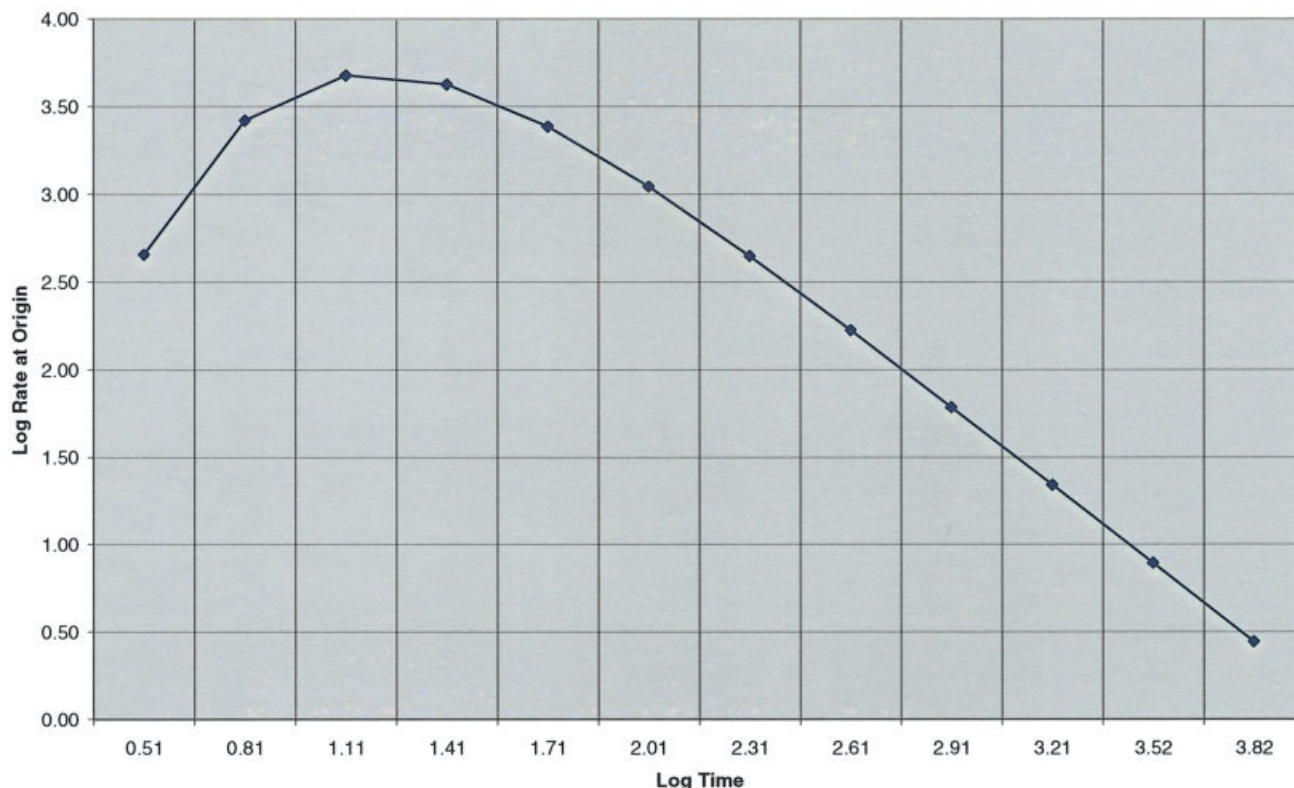


**Figure 12** Time dependence of rate. [Color figure can be viewed in the online version, which is available at [www.interscience.wiley.com](http://www.interscience.wiley.com).]

the half separation distance. The periodicity is represented in Figure 11. The arrow represents the origin where the oxide ion is located at all times. The region on each side of the origin has no epoxy rings as they have been depleted from another mechanism operating at a faster rate. This region is  $-A$  to  $+A$ . At  $A$ , the initial content of the epoxy ring jumps instantaneously to its normal value,  $M_0$ , and continues to  $-B$  and  $+B$ . Extending the model in either direction repeats the sequence in a periodic fashion. The mathematical expression for the arrival rate of an epoxide ring at the origin is  $dM/dt = D d^2M/dx^2$  at  $x = 0$ . The arrival rate comes from both directions and to not have an accumulation at the origin, one side is designated as  $-M_0$ . This formulation emulates the physical occurrence where the epoxide ring is opened and destroyed. As time is increased the arrival rate builds up as epoxide rings traverse the region  $A$  and then diminishes as the region,  $B$ , depletes.

The rate model consists of a linear combination of four error functions involving dimensional parameters,  $A$  and  $B$ . The rate is evaluated at the origin. Figure 12 shows a representation of the rate at the origin as a function of time on a log–log basis. The terms are in arbitrary units as the diffusion coefficient is a scaling parameter not known initially. The rate

increases as expected as the epoxy rings arrive at the origin for reaction with oxide ion. The rate reaches a maximum and then diminishes after the epoxy content is depleted appreciably. The depletion phase follows the familiar  $3/2$  power with time similar to what was found in the thesis.

The model allows for adjustment in the rate due to depletion of the zone,  $A$ , by a more rapid reaction mechanism. If  $A = 0$  then there is no depletion. As  $A/B$  approach unity, the rapid reaction mechanism is responsible for most of the epoxy ring opening and less is available by the diffusion mechanism. Figure 13 illustrates this behavior where the value  $A/B$  is expressed in terms of the available epoxy for reaction by the diffusion process. When  $A/B = 0$  then the available epoxy is unity. As  $A/B$  approaches 1 the available epoxy diminishes toward 0. It is seen that as the available epoxy increases the maximum rate of arrival at the origin increases and the time of the maximum gets shorter. All the relationships are shown in arbitrary units.

The purpose of this exercise is to determine how much the diffusion mechanism contributes to the overall reaction rate. The late stages of reaction show a  $3/2$  power dependence on time. The model can be scaled to satisfy the experimental heat rate in the late

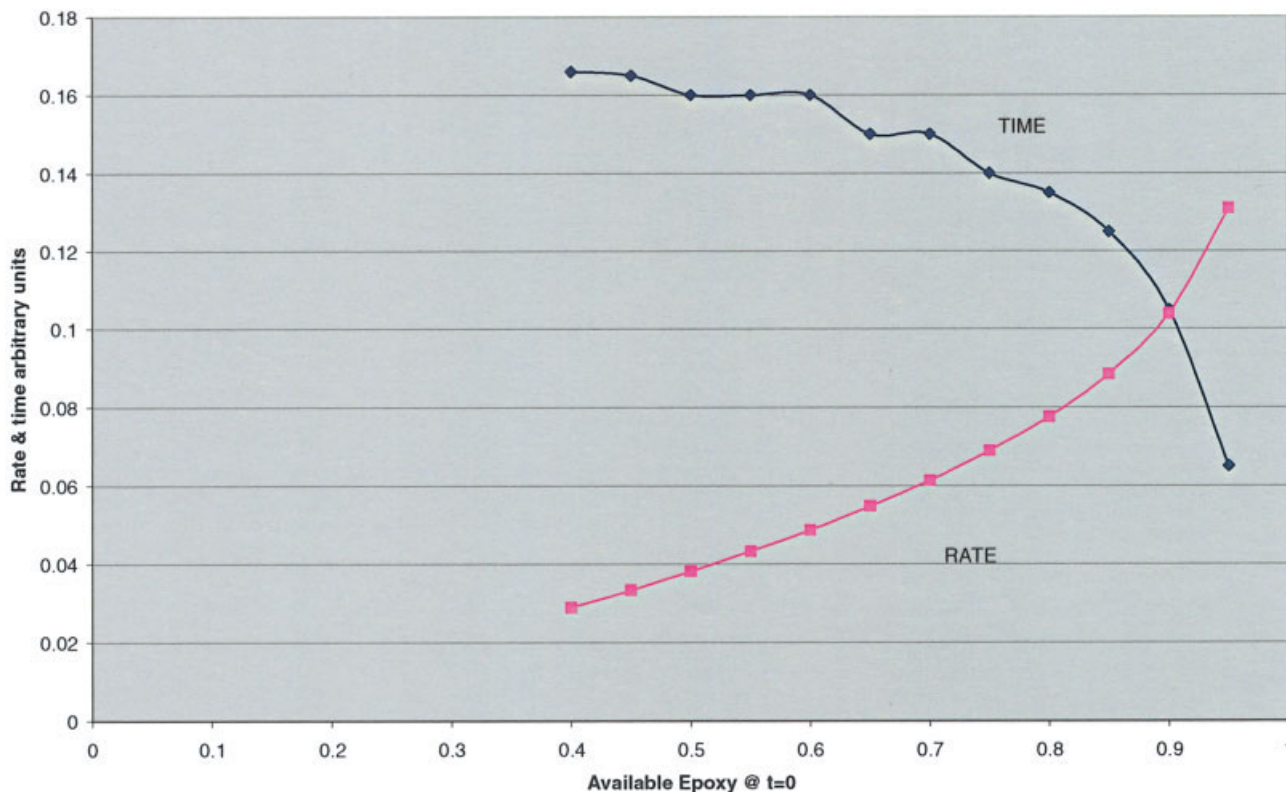


**Figure 13** Times and rates at max condition. [Color figure can be viewed in the online version, which is available at [www.interscience.wiley.com](http://www.interscience.wiley.com).]

stages and then back extrapolated to determine its contribution in the early phases of reaction particularly the accelerating phase. The result will be shown in a later section but it is evident that such an extrapolation can not explain the experimental heat rates in the early stages and contributes only in a minor way.

### MODEL DEVELOPMENT AND CURVE FITTING

The results discussed so far cover the initial and final phases of the polymerization process but the amine reaction and the diffusion mechanisms proposed account for only about 20% of the heat generated. The middle region of the heat rate curve shows a very symmetrical pattern about the time at maximum after subtracting the initial and final stages. Also as shown Figure 5, the heat rate is very symmetrical about the 50% completion point. Inspection of the results suggests that a Gaussian type reaction rate mechanism is dominant. To test this hypothesis, the experimental results were compared to a calculated heat rate combining the heat rate from the amine reaction, the diffusion process and a Gaussian term. The amine reaction was computed using the parameters described earlier. The diffusion process parameters described under the section

*Discussion and Analysis of the Decelerating Phase* were computed using the late stage experiment results to set their values. The parameters for the Gaussian curve were set by making the total calculated heat rate as close to the experimental heat rate as possible. The Gaussian parameters will be discussed first, then the comparison with the experiments will follow and then a possible mechanism that fits the mathematical features is proposed.

#### The Gaussian model

The basic expression is as follows:

$$Y = Y_{\max} \text{Exp} - ((x_{\max} - x) / \sigma)^2 \quad (3)$$

where  $Y$  and  $x$  are generalized variables of a bell-shaped curve about a median or peak. If (3) is applied to the data in Figure 5 in which all three experiments coincide in a universal curve,  $Y/Y_{\max}$  becomes the ratio of observed heat rates,  $dH/dt$ , and  $x$  is the fraction of heat evolved,  $\int d(H/H_0)/dt$ .  $H_0$  is the total heat evolved in the experiment. Since the maximum rate occurs at a heat fraction of 0.5 then the  $x$  term becomes  $(0.5 - \int dH/dt)$ . Application of eq. (3) to Figure 5 indicates that the data fit very well except for the

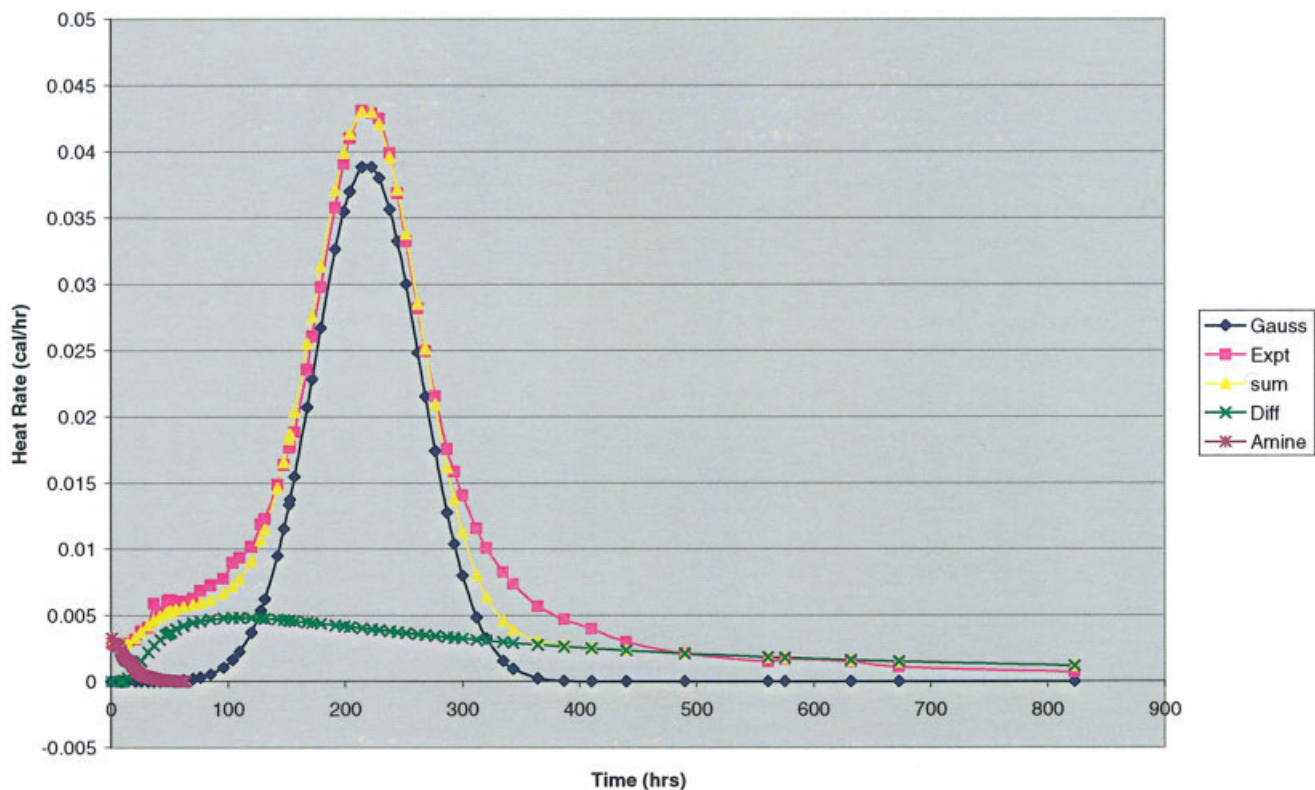


**Figure 14** Comparison of rates for Expt 034. [Color figure can be viewed in the online version, which is available at [www.interscience.wiley.com](http://www.interscience.wiley.com).]

extremes of the curve by choosing  $\sigma$  value of 0.35. The value represents a measure of the dispersion of the heat rate about the mean for all experiments regardless of the amine content. It indicates that the Gaussian reaction mechanism is universal.

Equation (3) may be applied to the individual experiments in a different way in which the  $x$  term becomes the time.  $t_{\max}$  is the time when the heat rate is a maximum.  $t$  represents the measured time during the experiment. Since (3) is going to be combined with the amine reaction and diffusion mechanisms, the  $Y_{\max}$  term must be modified slightly from the experimentally observed rate to allow for heat rates from these other mechanisms. The experimental  $Y_{\max}$  term will be reduced by a term,  $\Delta$ .  $\Delta$  and  $\sigma$  are determined by obtaining the overall best fit to the experimental data.

#### Comparison of the Gaussian mechanism with experimental data

Figures 14–16 show how the three reaction mechanisms fit with the experimental data. The calculated rates of heating were determined using a spreadsheet to follow the progress with time. The available epoxy, the unreacted amine and the oxygen ion contents were

computed at each measurement and the rates were updated according to the models used. A summary of the parameters used or calculated from the three reaction mechanisms is shown in Table VII. The heat rate contribution from the diffusion mechanism builds to its maximum value early in the experiment and then gradually tails off. This mechanism was forced to agree with the final experimental values late in the experiment which set the diffusion constant and scale factor to achieve such. No other mechanism is contributing to the heat rate in this final stage.

The heat rate contribution from reaction with the amine is over rather quickly in the 034 and 100 Experiments but persists in a small way throughout the 170 Experiment. In Table VII only a few percent of the initial amine content remains at the end. As expected the initial heat rate is generated by the amine reaction with the epoxy ring. In Experiment 034, an appreciable heat rate is generated by the diffusion mechanism in the early stage of the experiment. The bulge in the experimental data at about 50 h is replicated by the model calculation and appears to be due to the diffusion process. At this point the Gaussian mechanism has not begun as the oxide ion content has just barely reached the threshold for “ignition”. In Experiments



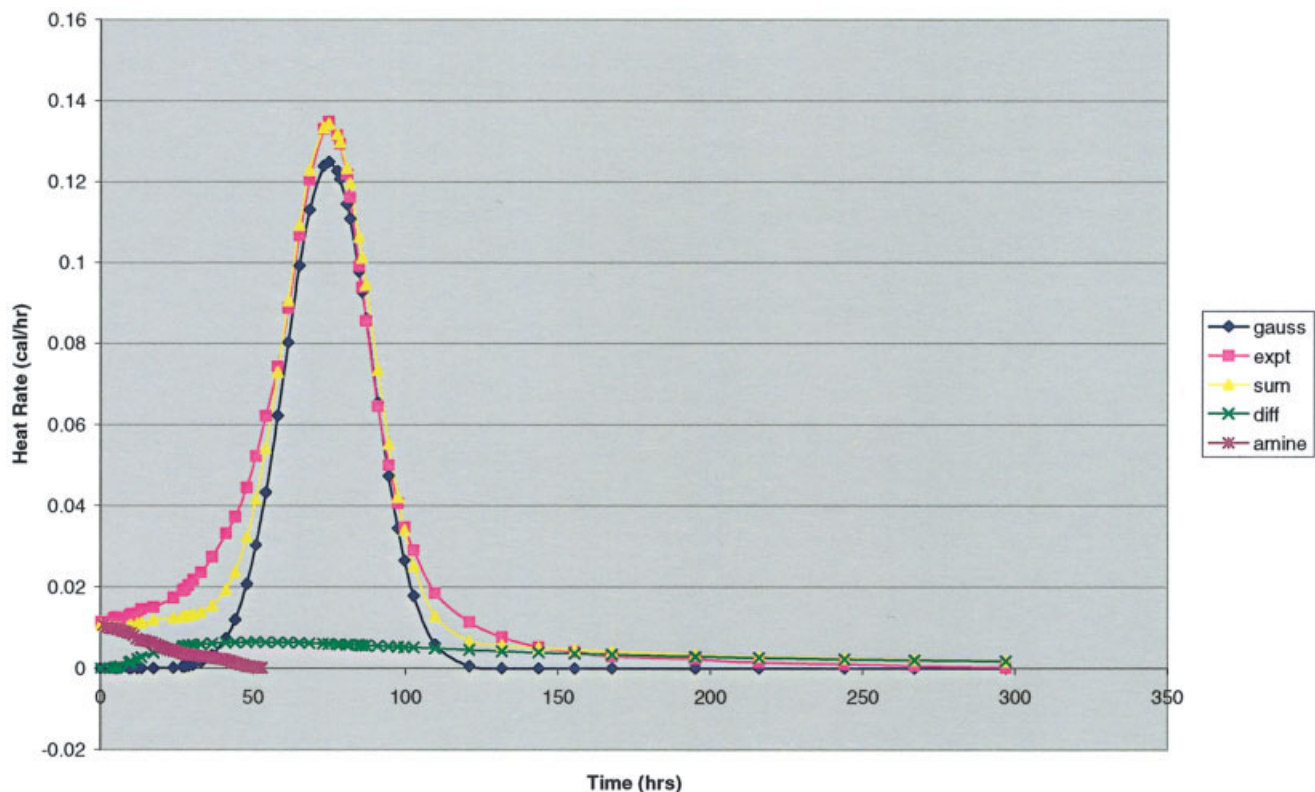


**Figure 15** Comparison of rates for Expt 100. [Color figure can be viewed in the online version, which is available at [www.interscience.wiley.com](http://www.interscience.wiley.com).]

100 and 170 “ignition” is well underway at the beginning and the diffusion process is less apparent in the composite calculated rate.

The Gaussian parameters were derived by subtracting the calculated amine and diffusion rates from the experimental heat rates at each measurement point and fitting the rest to a Gaussian curve derived in Section *Discussion and Analysis of the Decelerating Phase*. The two parameters,  $\sigma$  and  $\Delta$  are shown in Table VII. They were adjusted systematically to obtain the lowest standard of error from the experimental results. The calculated heat rates from the Gaussian mechanism are shown in Figures 14–16. By summing all three heat rate mechanisms, the result is very close to the experimental data except at the lower shoulder of the peaks in all the experiments. This difference accounts for only about ten percent of the total heat generated and is consistent with the calculated remaining epoxy at the end of the experiment as shown in Table VII.

The ratio,  $t_{\max}/\sigma$ , appears to be about the same in all three experiments, an indication that the Gaussian mechanism is universal. There is a reasonable linear relationship between the heat rate at  $t_{\max}$  and the oxide ion content at that point.

#### Proposed physical features associated with the Gaussian mechanism

Earlier it was shown that the oxide ion content had to reach a certain level to “ignite” the propagation step. Thereafter the reaction rate accelerated more than what would be expected by oxide ion growth. Therefore the electron mobility must be enhanced by the chemical potential field. Volume resistivity measurements were made by Warfield and Petree<sup>6</sup> where they assumed that the polymerization rate was proportional to the maximum rate of change of the logarithm of the resistance. Activation energies of the order of 17 kcal were found and the 14,000 cal per equivalent epoxy for the aliphatic/polyamine system studied. Dannenburg and Harp<sup>7</sup> studied the polymerization of EPON 828 with piperidine as the initiator at concentrations similar to Experiment 100. They worked at temperatures of 65 degrees C and above. The epoxy content was followed spectrophotometrically and chemically. After about 15 h, the reaction stopped with a conversion of 78–80%. Continued heating to higher temperatures did not remove all the residual epoxy. They showed a linear drop in the epoxy content with time. Details on the rate of reaction were difficult to determine from this type of experiment.

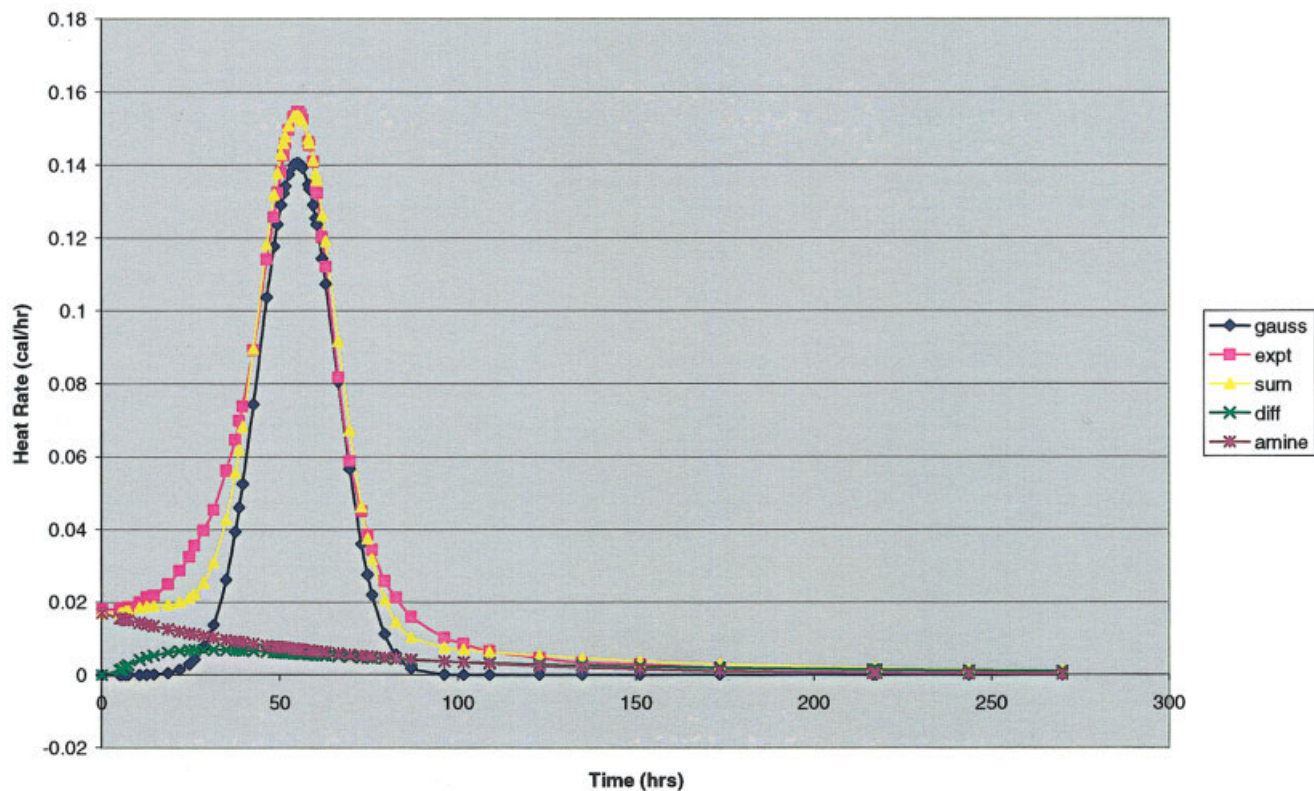


**Figure 16** Comparison of rates for Expt 170. [Color figure can be viewed in the online version, which is available at [www.interscience.wiley.com](http://www.interscience.wiley.com).]

However, if one applies the 17 kcal activation energy to this composition to determine the termination point at 27°, about 300 h is required, which would be in agreement with the termination point for Experiment 100.

Thus it can be expected that the electron associated with an opened epoxy ring will seek a suitable location for another opening. The distance of influence is about 25 Å assuming a cubic array of ions. The ions are floating in a sea of epoxy groups initially about 7 Å apart. Therefore about 50 epoxy cells could be under the influence of the potential field at "ignition". Since they do not all react at once there must be a restraining condition.

The peaking of the reaction rate at 50% completion indicates that a product of the reaction (ether linkage) is a restraining condition. The maximum rate occurs when there is an equal abundance of reactant and reaction product. The reaction product is the COC ether group. The open epoxy ion,  $\text{CO}^-$ , an unopened epoxy ring and an ether group combine to form a reaction complex. Any one of these entities may be viewed as occupants of a cell. The oxide ion is the core cell. Its nearest neighbor cells can contain any one of the three entities. Since the oxide ion is the least abundant it does not often

occupy nearest neighbor cells. Therefore the condition for reaction is that the nearest neighbor cells should contain one epoxy ring and one ether group. The probability of this occurrence is greatest at the 50% point. The reaction rate rises up to this point and diminishes beyond this point. A pictorial representation of the reaction complex is shown in Figure 17 together with the Epon 828 molecule. A possible hexagonal arrangement is shown from the three participating components.

#### Refinements to the Gaussian model

Many text books on statistical mechanics discuss how the Gaussian relationship is used in probabilistic theory. The probability that two entities will be found adjacent to each other in a large group depends on the number of trials involved. The gauss relationship used above applies when there are a large number of trials. When the number of trials decreases then the probability curve broadens. This phenomenon is applied here using the derivation from Margenau and Murphy.<sup>8</sup> The term,  $\sigma$ , used above is replaced by a term dependent on the number of trials,  $n$ . Equation (3) is replaced by eq. (4),



TABLE VII  
Parameters Used and Observations From Rate Model Calculations

Parameter	Experiment		
	034	100	170
Diffusion parameters			
A/B	0.632	0.632	0.632
Available epoxy	0.95	0.95	0.95
Oxide ion spacing at $t = \infty$ , $A^0$	21.4	15.0	12.6
Effective diffusion constant, $D$	1.19E-3	3.57E-3	7.13E-3
Scale factor to fit experimental data	1/30	1/15	1/7
Amine/oxide ion parameters			
Amine rate constant, $k$	1.65E-2	1.65E-2	1.65E-2
Oxide ion equilibrium constant, $K$	0.0215	0.0215	0.0215
Ratio OH/ Epoxy equivalents at $t = 0$	0.1	0.1	0.1
Oxide ion equivalents at $t = 0$	0.39E-5	0.68E-5	0.80E-5
at $t = t_{\max}$	1.72E-5	3.85E-5	5.08E-5
at $t = \infty$	1.80E-5	5.24E-5	8.06E-5
Amine equivalents at $t = 0$	1.80E-5	5.3E-5	8.16E-5
at $t = t_{\max}$	1.72E-5	1.84E-5	3.61E-5
at $t = \infty$	0.013E-5	0.14E-5	0.193E-5
Gaussian parameters			
Time at maximum rate, $t_{\max}$ (h)	214.7	74.8	55
Dispersion parameter, $\sigma$ (h)	64.5	20	15.4
Ratio $t_{\max}/\sigma$	3.33	3.74	3.57
Epoxy equivalents, at $t = 0$	5.3E-4	5.3E-4	4.8E-4
at $t = \infty$	0.51E-4	0.79E-4	0.61E-4
Heat output/Equiv epoxy (cal)	14000	14000	14000
$dH/dt$ at $t = t_{\max}$ (cal/h)	0.043	0.135	0.155
Rate adjustment at $t = t_{\max}$ , $\Delta$ (cal/h)	0.004	0.01	0.014

$$Y = Y_{\max}(1/\sqrt{2\pi npq})(\text{Exp}-(nq/2p(t/t_{\max}-1)^2)) \quad (4)$$

where  $p$  and  $q$  represent the probability that an epoxy group and a reacted ether group are located

in a given cell. The presence of an open epoxy ion is small so that  $p + q \approx 1$ . For two adjacent cells to be found in an array of cells each containing an epoxy group and an ether group, then  $p = q = 1/2$ . Since

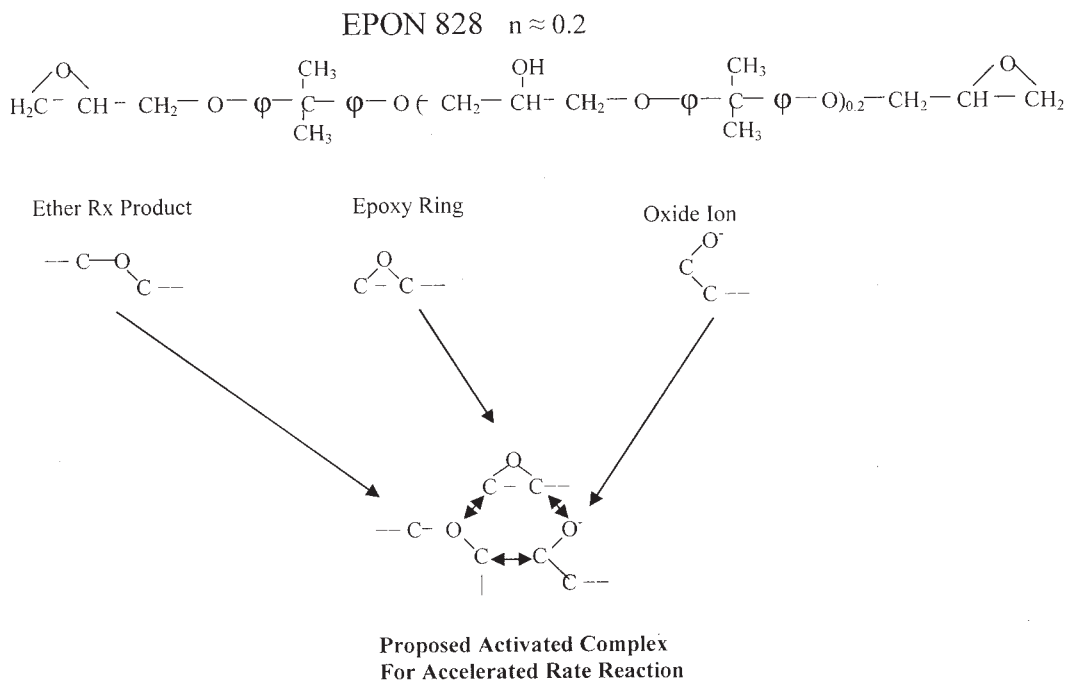


Figure 17 Proposed activated complex for accelerated rate reaction.

$n$  appears both in the coefficient and the exponent, and the result is fixed relative to the time of maximum heat rate,  $Y_{\max}$  is renormalized after each  $n$  to be equivalent to the experimental heat rate at maximum after allowing for an adjustment in the  $\Delta$  term described above.

Recalculation of the heat rate from the proposed Gaussian mechanism by varying  $n$  [eq. (4)] instead of  $\sigma$  [eq. (3)] and by comparing the overall fit with the experimental data, the lowest standard of error occurred at  $n = 20, 24,$  and  $24$  for Experiments 034, 100, and 170 respectively. The errors were about an order of magnitude less than the errors obtained with eq. (3) and shown in Figures 14–16. Therefore incorporating the number of trials in the Gaussian mechanism improves the fit of the model to the experimental data.

An interesting outcome of this refinement is that best fit values of  $n$  are about one half the number of epoxy cells in the array of a larger cell where the oxide ion content is sufficient to “ignite” the accelerated reaction mechanism. An electron from an opened epoxy after ignition has about 50 epoxy cells to sample after ignition, but it would be limited to about 25 trials as it is looking for an adjacent cell pair containing one unopened epoxy group and one ether group.

No evidence of this mechanism was found in a review of the literature on the reaction kinetics of epoxide polymerization. One experiment was cited anecdotally that no reaction was observed in the first few hours but when left for a few days it gelled into a clear solid. The amine was below the stoichiometric level similar to the experiments in this paper. Tanaka (see Ref. 3 Paper 14) reported on a modified epoxy with vinyl groups to develop self crosslinking. Pyridine was used to promote opening of the epoxide group. Using a spectrophotometric method, he showed that the rate of disappearance of the epoxy group reached a maximum at 50% reaction similar to that found in this paper. The rate peaks were more prominent as the pyridine content was increased. The ratios of pyridine to epoxy were below stoichiometric values but much higher than that used in this paper. From the fact that tertiary amines (pyridine) are weaker bases than secondary amines (piperidine) it is not surprising that higher ratios would be required. The peak rates were up to two times the initial rate indicating the accelerating effect is not as dramatic as observed in this paper.

Another possible accelerating reaction rate might be inferred from a paper by Crivello and Lam (see Ref. 3 Paper 1). This paper examined photoinitiated cation polymerization of epoxy resins. The mechanism involves a cationic environment after exposure to ultraviolet light. The results indicate that the propagation which follows a short pulse of light continues long

after the radiation. The intensity of the light must achieve a certain threshold to sustain the reaction which might indicate that the cation level must reach a certain concentration to ignite the propagation. The rate studies reported do not enable one to determine if this is equivalent to an “ignition” as observed in this paper.

There are a few questions that need to be answered before going further with the mechanistic description. They are:

- The heat of reaction difference between the epoxy reaction with an amine and with an oxide ion.
- The total heat from Experiment 034 was higher than the others and the maximum rate occurred at 44% completion. A higher heat of reaction for the amine could explain this result.
- The influence of ether like reaction product groups versus the influence of two phenolic linkage in the EPON 828 molecule?
- The ether group fits the results very well, but why doesn't an abundance of phenoxy groups already there at the start have an influence?
- The residual unreacted epoxy groups, if any, after termination of the experiment.
- The literature cites many studies where there is residual epoxy even after continued heating. The calorimetric experiments gave no evidence but the residual epoxy content was never determined chemically and spectrophotometrically.

## SUMMARY AND CONCLUSIONS

Epoxide polymerization reactions where the amine content is below the stoichiometric ratio have a more complex set of mechanisms than have been shown in the literature for stoichiometric reactions. The data set of heat rates reveals details often lost by following extent of reaction rather than the rate. Diffusion of reacting species makes a small but measurable contribution to the heat output. The amine reaction and hydrogen ion exchange with embedded hydroxyl groups explained how ionic system could reach and maintain a threshold oxide ion content that enabled “ignition” and accelerate the reaction rate based on statistical arguments. The analyses suggest that a complex of functional groups must coalesce in a statistical fashion to enable heat rate peaking. The complex proposed is an oxide ion formed from opening an epoxy ring, an unopened epoxy ring, and a reaction product having an ether bond. The ether bond grows in and stimulates the acceleration of the rate. After 50% completion of the reaction, the available unopened epoxy rings become depleted and reduce the reac-

tion rate. Finally only the diffusion mechanism is left to generate heat for situations where the reactants are too far apart for the statistical mechanism to operate.

### References

1. Aitken, E. Ph.D. Dissertation, University of California, Los Angeles, 1954.
2. Epoxy Resins; May, C. A., Tanaka Y., Eds.; Dekker: New York, 1973; Chapter 3.
3. Epoxy Resin Chemistry; Bauer, R. S., Ed.; ACS Publications: Washington, DC, 1979.
4. Epoxy Resins II; Bauer, R.S., Ed.; ACS Publications: Washington, DC, 1983.
5. Kenyon, W.; Tong, L. J Am Chem Soc 1949, 71, 1925.
6. Warfield, R. W.; Petree, M. C. SPE Trans 1961, 1, 3.
7. Dannenburg, H.; Harp, W. R. Anal Chem 1956, 28, 86.
8. Margenau, H.; Murphy G. M. The Mathematics of Physics and Chemistry; Van Nostrand: New York, 1943, p 415.